# Correlation Between Severity of Pulmonary Arterial Hypertension and $^{123}$I-Metaiodobenzylguanidine Left Ventricular Imaging

Fumio Sakamaki, Toru Satoh, Noritoshi Nagaya, Shingo Kyotani, Hideo Oya, Norifumi Nakanishi, Sachio Kuribayashi, and Yoshio Ishida

*Departments of Medicine and Radiology, National Cardiovascular Center, Osaka, Japan*

It remains unclear whether cardiac sympathetic nervous function is disturbed in patients with pulmonary arterial hypertension (PH) and how sympathetic dysfunction is related to PH. **Methods:** In this study, $^{123}$I-metaiodobenzylguanidine (MIBG) imaging of the heart, which reveals the sympathetic innervation of the left ventricle, was performed in 7 healthy volunteers without cardiopulmonary disease (control subjects); 55 patients with PH, including 27 with chronic thromboembolic pulmonary hypertension (CTEPH) of major vessels; and 28 patients with primary pulmonary hypertension (PPH). **Results:** Cardiac $^{123}$I-MIBG uptake, assessed as the heart-to-mediastinum activity ratio (H/M), was significantly lower in the CTEPH and PPH groups compared with that in the control group ($P < 0.01$). Myocardial MIBG turnover, expressed as the washout rate (WR [%]) from 15 to 240 min, was significantly higher in the CTEPH and PPH groups than that in the control group ($P < 0.01$). In the PPH group, H/M and WR values of MIBG correlated with the severity of pulmonary hypertension (represented by total pulmonary vascular resistance determined by right heart catheterization), the right ventricular ejection fraction determined by electron beam CT, and other variables but did not correlate well in the CTEPH group. In both groups, patients with H/M $\geq$ 2.0 showed better cumulative survival than did those with H/M $<$ 2.0 ($P <$ 0.05). **Conclusion:** Patients with PH have significant left ventricular myocardial sympathetic nervous alteration. $^{123}$I-MIBG imaging of the heart is useful for assessing the severity of pulmonary hypertension caused by PPH or CTEPH.

**Key Words:** pulmonary hypertension; sympathetic nervous system; $^{123}$I-metaiodobenzylguanidine

**J Nucl Med 2000; 41:1127–1133**

Both chronic thromboembolic pulmonary hypertension (CTEPH) and primary pulmonary hypertension (PPH) are associated with severe pulmonary arterial hypertension (PH) and right ventricular (RV) pressure overload, leading to RV failure and grave morbidity and mortality (*1,2*). Right heart catheterization is the best method to determine the severity and prognosis of patients with PH but is invasive and has some risks in patients with PH. Noninvasive methods to assess the severity of PH and the effects of various therapies are needed in the management of patients with CTEPH or PPH.

Few investigations have been performed to clarify whether the cardiac sympathetic nervous system is disturbed in patients with PH, whereas sympathetic denervation has been shown to be associated with myocardial ischemia, cardiomyopathy, and other heart diseases in which left ventricular (LV) function is disturbed. Furthermore, it remains unclear whether LV sympathetic nervous dysfunction may reflect the severity and outcome of PH.

Metaiodobenzylguanidine (MIBG), an analog of guanethidine, shows similarity to norepinephrine (NE) with regard to neuronal transport and storage in systemic nerve endings (*3,4*). $^{123}$I-MIBG imaging of the heart can assess efferent adrenergic neuronal function and integrity of the left ventricle (*5,6*). Abnormal $^{123}$I-MIBG imaging findings have been reported in ischemic heart disease (*7*), aortic stenosis (*8*), congestive cardiomyopathy (*9*), and transplanted hearts (*10*).

In patients with PH, LV sympathetic dysfunction could result from direct LV damage by the right ventricle through the interventricular septum and from the influence of systemic sympathetic overactivity. Therefore, this study was undertaken to investigate whether LV sympathetic nervous function, assessed by the uptake and washout of $^{123}$I-MIBG, is disturbed in patients with PPH and CTEPH compared with that in healthy volunteers (control subjects) and to assess the usefulness of $^{123}$I-MIBG imaging in managing patients with CTEPH or PPH by evaluating the correlation between abnormality of $^{123}$I-MIBG imaging findings and the severity of PH.

Received Jul. 6, 1999; revision accepted Oct. 27, 1999.

For correspondence or reprints contact: Fumio Sakamaki, MD, Division of Cardiology, Department of Medicine, National Cardiovascular Center, 5-7-1 Fujishirodai, Suita, Osaka 565-8565, Japan.

## MATERIALS AND METHODS

### Patients

Fifty-five patients (21 men, 34 women; mean age ± SD, 51 ± 8 y; age range, 41–65 y) with PH were studied. All patients were in stable condition during this study protocol, and the series of examinations described in this study were performed within a 1-mo period. Treatment was unchanged during the study period. No patients were receiving any $\alpha_1$ blockers or suffered from hypertension, diabetes mellitus, pheochromocytoma, or Shy-Drager syndrome. PH was defined as a mean pulmonary artery pressure of >20 mm Hg at rest. The patients consisted of 27 subjects with CTEPH (13 men, 14 women; mean age, 55 ± 12 y; age range, 21–72 y) and 28 with PPH (8 men, 20 women; mean age, 38 ± 13 y; age range, 20–64 y). CTEPH was identified by conventional perfusion lung scanning using $^{99m}$Tc-macroaggregated albumin and pulmonary angiography (*11*). PPH was diagnosed as pulmonary hypertension unexplained by any secondary cause on the basis of the criteria of the National Institutes of Health registry on PPH (*12*). Patients with 1 or more of the following conditions were excluded: significant LV disease, such as cardiomyopathy, coronary artery disease, or mitral or aortic valvular disease; acute heart failure; chronic renal impairment (serum creatinine level, >133 μmol/L); and sustained arrhythmia, such as atrial fibrillation. $^{123}$I-MIBG imaging was also performed in 7 healthy volunteers (6 men, 1 woman; mean age, 47 ± 15 y; age range, 27–68 y) without cardiopulmonary disease who served as the control group. All subjects were given an explanation of the purpose of the study and provided written informed consent.

### Protocol for $^{123}$I-MIBG Imaging

After thyroid blockade with 30 mg potassium daily from the day before $^{123}$I-MIBG imaging until the day after the study, a dose of 111 MBq $^{123}$I-MIBG (Daiichi Radioisotope Laboratory, Tokyo, Japan) was administered intravenously. Anterior planar and SPECT images of the heart were acquired at rest 15 min after (early imaging) and 4 h after (delayed imaging) administration using a triple-head gamma camera (MULTISPECT 3; Siemens Medical Systems, Iselin, NJ) equipped with a low-energy, high-resolution collimator. Anterior planar images were acquired for 180 s and recorded on a 512 × 512 matrix. SPECT images were acquired by 360° camera rotation with 36 views for 40 s and recorded on a 64 × 64 matrix. The data were reconstructed by filtered backprojection, and oblique tomographic slices in the short, vertical long, and horizontal long axes were computed and displayed.

### Data Analysis of $^{123}$I-MIBG Uptake

Regions (10 × 10 mm$^2$) of interest (ROIs) were placed manually on the whole heart and on the upper mediastinum in the anterior planar image. The mean $^{123}$I-MIBG counts of the heart from the early image (He) and from the delayed image (H) were calculated. The mean mediastinal count was obtained from the early image (Me) and from the delayed image (M). The heart-to-mediastinum count ratio was calculated for the early image (He/Me) and for the delayed image (H/M). H/M was used as the final index of myocardial uptake of MIBG. In addition, the washout rate (WR) of $^{123}$I-MIBG from the heart for 4 h was determined according to the formula: $WR (\%) = [(He - Me) - (H - M)] \times 100/(He - Me)$.

Cardiac $^{123}$I-MIBG distribution was assessed using the short-axis SPECT image at the midventricular level. The short-axis tomogram of the left ventricle in the delayed image was divided into 6 regions by visual inspection as shown in Figure 1. An ROI of 2 × 2 pixels was placed over the center of each region by manual drawing to measure regional $^{123}$I-MIBG uptake. The mean $^{123}$I-MIBG count per 2 × 2 pixels was measured in each region. The relative regional uptake (RRU [%]) was determined in each region as the ratio of the regional uptake per pixel to the maximum uptake in the 6 regions.

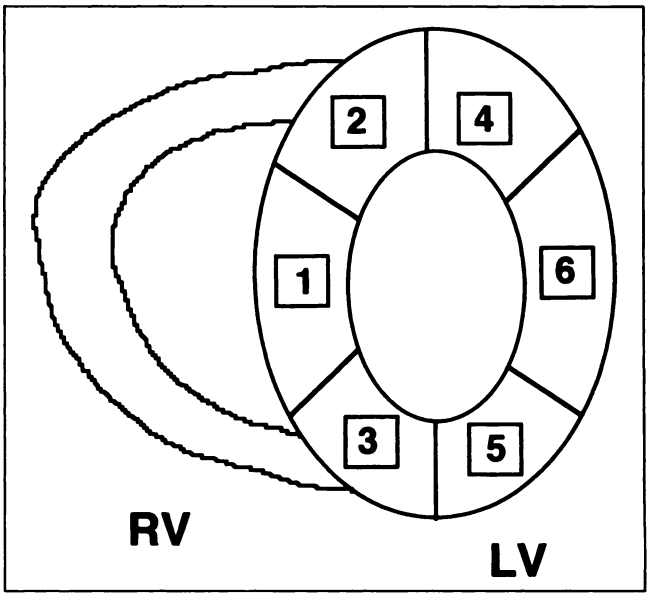


**FIGURE 1.** Schema of short-axis tomogram at midventricular level shows deformed left ventricle (LV) and expanded right ventricle (RV) associated with pulmonary hypertension. LV is divided into 6 regions. Myocardial ROI segment was drawn manually in each region: septal (1), anteroseptal (2), posteroseptal (3), anterolateral (4), posterolateral (5), and lateral (6). Square ROI of 2 × 2 pixels was placed over center of each of 6 regions to measure regional $^{123}$I-MIBG uptake.

### Hemodynamic Studies

In the CTEPH and PPH groups, right heart catheterization was performed after an overnight fast. Four hemodynamic variables were obtained at end-expiration: mean right atrial pressure (mRAP), mean pulmonary arterial pressure (mPAP), pulmonary capillary wedge pressure, and mean systemic arterial pressure. Cardiac output (CO) was determined by the Fick method. Total pulmonary resistance (TPR) was calculated by dividing mPAP by CO. Standard spirometry was also performed in both groups (*13*).

### Electron Beam CT of Heart

Electron beam CT was performed with a C-150XP scanner (Imatron, Inc., South San Francisco, CA) as reported (*14–16*). Briefly, cine mode scanning (scanning time, 50 ms for images recorded on a 256 × 256 matrix) was performed after administration of 40–50 mL nonionic contrast medium (Iopamidol 370; Nippon Schering, Osaka, Japan). The scanner table was rotated 25° in a clockwise horizontal direction to obtain near short-axis views of the heart. Eight-level (10 contiguous images/level) cine mode scans of the heart were obtained with electrocardiographic gating. The end-diastolic (R wave on electrocardiogram) and end-systolic (smallest ventricular chamber volume during the cardiac cycle) frames were identified at each tomographic level. Endocardial and epicardial borders of the ventricles were determined using previously described methods of edge detection for electron beam CT

**TABLE 1**
Pulmonary Hemodynamic and Respiratory Function Data of Patients in CTEPH and PPH Groups

| Parameter | CTEPH (n = 27) | PPH (n = 28) |
|---|---|---|
| mRAP (mm Hg) | 4.6 ± 4.1 | 7.0 ± 4.1* |
| mPAP (mm Hg) | 44.0 ± 12.7 | 58.4 ± 14.0* |
| CO (L/min) | 3.7 ± 1.1 | 3.3 ± 1.4 |
| TPR (Wood units) | 14.0 ± 7.0 | 20.4 ± 8.3* |
| RVEF (%) | 32.3 ± 12.3 | 33.8 ± 13.8 |
| LVEF (%) | 55.9 ± 12.2 | 56.0 ± 9.6 |
| $Pa_{O_2}$ (T) | 61.2 ± 9.6 | 69.3 ± 13.3* |
| $AaD_{O_2}$ (T) | 46.3 ± 14.3 | 41.2 ± 15.5 |

*$P < 0.05$ vs. CTEPH group.
$AaD_{O_2}$ = alveolar arterial difference of oxygen.
Values are mean ± SD.

(*14,15*). A modified version of Simpson's method was used in multisection cine mode scans to obtain the volume of both ventricles, and the RV ejection fraction (EF) and LVEF were then calculated (*16*).

### Assay for Plasma NE

Blood samples were drawn from the antecubital vein in the morning while subjects were awake and on bed rest. Blood was immediately transferred into a glass tube containing disodium ethylenediaminetetraacetic acid (1 mg/mL) and centrifuged at 4°C. Plasma NE concentration was measured by high-performance liquid chromatography to evaluate the systemic sympathetic nervous activity.

### $^{123}$I-MIBG Imaging and Outcome

To assess the correlation between survival of patients with PH and the results of $^{123}$I-MIBG imaging, the subjects were divided into 2 groups; those with H/M ≥ 2.0 and those with H/M < 2.0. Patients in the CTEPH group consisted of 13 subjects with H/M ≥ 2.0 (7 men, 6 women; mean age, 51 ± 14 y; age range, 21–70 y) and 14 with H/M < 2.0 (6 men, 8 women; mean age, 58 ± 10 y; age range, 38–72 y). Patients in the PPH group consisted of 12 patients with H/M ≥ 2.0 (1 man, 11 women; mean age, 32 ± 11 y; age range, 20–49 y) and 17 with H/M < 2.0 (7 men, 10 women; mean age, 43 ± 13 y; range, 23–64 y). All patients were monitored for at least 6 mo after $^{123}$I-MIBG imaging. The primary endpoints included death from all causes, thromboendarterectomy in CTEPH patients, and introduction of continuous intravenous prostacyclin (epoprostenol) therapy in PPH patients.

### Statistical Analysis

All data were presented as mean ± SD. Differences in hemodynamic parameters between the CTEPH and PPH groups were analyzed using the Mann-Whitney *U* test. Differences in H/M and WR of $^{123}$I-MIBG imaging, plasma NE level, and RRU of $^{123}$I-MIBG among the control, CTEPH, and PPH groups were analyzed using 1-way ANOVA and Fisher's least-significant difference test (Stat View; SAS Institute, Inc., Cary, NC). Simple regression analysis was used to correlate $^{123}$I-MIBG findings with hemodynamic parameters and ventricular EF determined by electron beam CT. A cutoff value of $P < 0.05$ was used for detection of statistically significant differences.

Kaplan-Meier curves were constructed for the 2 patient groups divided by an H/M value of 2.0 and evaluated separately for the CTEPH and PPH groups. Differences in survival between the 2 groups were examined by a log-rank test and proportional-hazards regression analysis.

## RESULTS

Results of pulmonary hemodynamic studies and respiratory function tests in the CTEPH and PPH groups are given in Table 1. Patients in the PPH group had higher mRAP, mPAP, and TPR, whereas those with CTEPH had lower $Pa_{O_2}$ ($P < 0.05$).

H/M and WR in $^{123}$I-MIBG images in control, CTEPH, and PPH groups are presented in Figure 2. H/M in the CTEPH group (1.93 ± 0.42) and the PPH group (1.95 ± 0.35) was significantly lower than that in the control group (2.49 ± 0.16; $P < 0.05$). WR in the CTEPH group (40.9 ± 17.9) and the PPH group (41.5 ± 13.3) was significantly higher than that in the control group (22.3 ± 3.9; $P < 0.01$). The mean $^{123}$I-MIBG uptake count in the septal and posteroseptal region was lower in patients in the CTEPH and PPH groups than in patients in the control group. Septal, anteroseptal, posteroseptal, and posterolateral RRU of $^{123}$I-MIBG was significantly lower in patients with CTEPH and PPH compared with that in control subjects (Table 2). Two representative cases of $^{123}$I-MIBG SPECT imaging (bull's-eye display) in the PPH group are presented in Figure 3.

The relationships between pulmonary hemodynamic parameters and $^{123}$I-MIBG imaging parameters are presented in Table 3. In the PPH group, most of the hemodynamic parameters, except mRAP, were significantly correlated with $^{123}$I-MIBG parameters. On the contrary, in the CTEPH group, only mRAP and H/M and RVEF and WR were

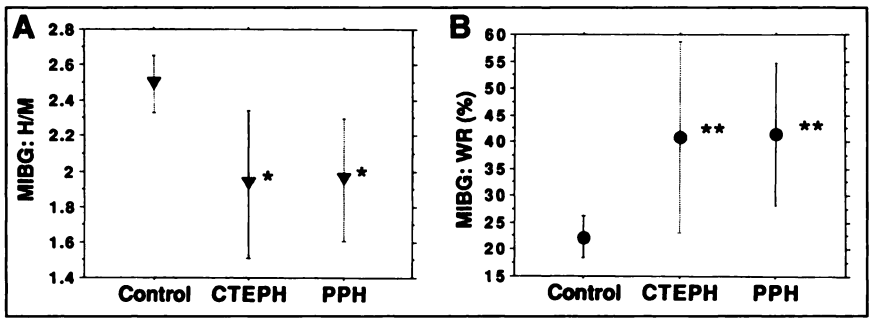


**FIGURE 2.** (A) Cardiac $^{123}$I-MIBG uptake is assessed as H/M (MIBG) in patients in control, CTEPH, and PPH groups. (B) Myocardial MIBG turnover is expressed as WR from 15 to 240 min (MIBG) in control, CTEPH, and PPH groups. Data are mean ± SD. H/M was significantly lower in CTEPH and PPH groups than in control group (*$P < 0.01$ versus control). WR was significantly higher in CTEPH and PPH groups than in control group (**$P < 0.05$ versus control).

**TABLE 2**
$^{123}$I Counts per Pixel in Each Region and RRU (%) of $^{123}$I-MIBG

| Area | Control | CTEPH | PPH |
|---|---|---|---|
| Septal | | | |
| Counts | 80 ± 25 | 61 ± 16 | 59 ± 11 |
| % | 93.4 ± 3.5 | 62.1 ± 15.5* | 60.0 ± 17.3* |
| Anteroseptal | | | |
| Counts | 82 ± 26 | 82 ± 21 | 83 ± 15 |
| % | 98.0 ± 2.1 | 86.1 ± 9.4* | 84.7 ± 12.1* |
| Posteroseptal | | | |
| Counts | 79 ± 25 | 58 ± 15 | 61 ± 11 |
| % | 92.9 ± 2.7 | 61.1 ± 14.0* | 61.8 ± 11.8* |
| Anterolateral | | | |
| Counts | 82 ± 29 | 93 ± 24 | 95 ± 17 |
| % | 98.9 ± 1.9 | 97.6 ± 3.5 | 96.9 ± 5.3 |
| Posterolateral | | | |
| Counts | 81 ± 26 | 80 ± 21 | 78 ± 14 |
| % | 97.3 ± 2.2 | 83.9 ± 12.2* | 79.5 ± 9.9* |
| Lateral | | | |
| Counts | 83 ± 27 | 92 ± 23 | 94 ± 16 |
| % | 99.3 ± 0.5 | 96.3 ± 5.6 | 95.7 ± 6.2 |

*$P < 0.01$ vs. control.

**TABLE 3**
Relationship Between Cardiopulmonary Function Data and Parameters of $^{123}$I-MIBG Imaging

| | *r* | | |
|---|---|---|---|
| Parameter | Total (n = 55) | CTEPH (n = 27) | PPH (n = 28) |
| mRAP (mm Hg) | | | |
| H/M | −0.31* | −0.43* | −0.28 |
| WR (%) | 0.27* | 0.33 | 0.22 |
| mPAP (mm Hg) | | | |
| H/M | −0.33* | −0.29 | −0.58† |
| WR (%) | 0.35* | 0.34 | 0.49* |
| CO (L/min) | | | |
| H/M | 0.37† | 0.24 | 0.52† |
| WR (%) | −0.40† | −0.27 | −0.57† |
| LVEF (%) | | | |
| H/M | 0.35* | 0.22 | 0.51* |
| WR (%) | −0.09 | −0.13 | −0.40 |
| RVEF (%) | | | |
| H/M | 0.56† | 0.41 | 0.71† |
| WR (%) | −0.54† | −0.47* | −0.64 |

*Statistically significant at $P < 0.05$.
†Statistically significant at $P < 0.01$.

significantly correlated. The relationships between TPR and $^{123}$I-MIBG imaging parameters are given in Figure 4 as representative data. In the PPH group, TPR was significantly correlated with H/M ($P < 0.001$; $r = -0.66$) and WR ($P < 0.001$; $r = 0.68$), whereas there was no significant correlation in the CTEPH group (H/M: $P = 0.16$, $r = -0.28$; WR: $P = 0.08$, $r = 0.34$).

The plasma NE concentration in the CTEPH group (420.0 ± 204.3 pg/mL) and the PPH group (404.5 ± 399.2) was significantly higher than that in the control group (68.9 ± 31.9; $P < 0.05$). Pulmonary hemodynamic parameters TPR, CO, $Pa_{O_2}$, and alveolar arterial difference of oxygen ($AaDo_2$) were correlated with the plasma NE concentration.

Fourteen patients survived in the CTEPH group, whereas 4 died of RV failure and 9 underwent thromboendartectomy during the 14 ± 10 mo of follow-up. Thirteen patients survived in the PPH group, whereas 7 died of RV failure and

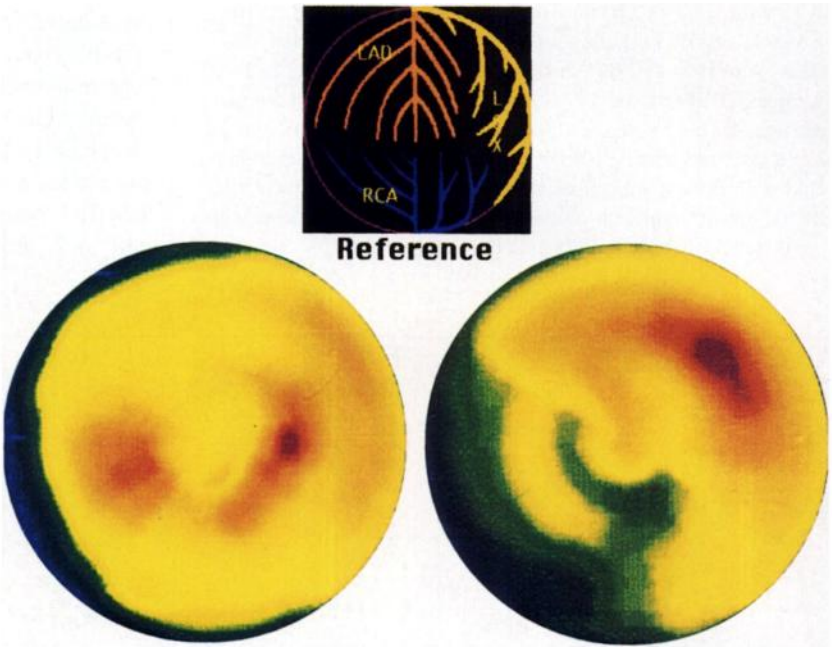


**FIGURE 3.** (Lower left) $^{123}$I-MIBG image (bull's-eye display) of mild PH case in 25-y-old woman in PPH group. mPAP and TPR were 22 mm Hg and 4.2 Wood units, respectively. On $^{123}$I-MIBG image, H/M was 2.25 and WR from 15 to 240 min was 23.9%. (Lower right) $^{123}$I-MIBG image of severe PH case in 27-y-old man in PPH group. mPAP and TPR were 77 mm Hg and 24.3 Wood units, respectively. On $^{123}$I-MIBG image, H/M was 1.78 and WR was 42%. Decreased $^{123}$I-MIBG uptake in myocardium is shown as green or blue color in region of interventricular septum in both patients and in inferior LV wall in 27-y-old man. (Top) Coronary arterial territory on short-axis image is shown. LAD = left anterior descending coronary artery; LCX = left circumflex coronary artery; RCA = right coronary artery.

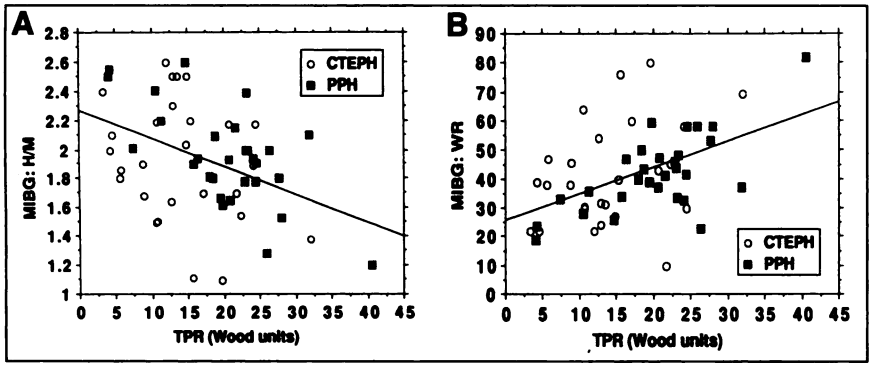


**FIGURE 4.** Correlations of H/M (A) and WR (B) of $^{123}$I-MIBG image with TPR in CTEPH (○) and PPH (■). TPR was significantly correlated with H/M ($r = -0.66$; $P < 0.001$) and WR ($r = 0.68$; $P < 0.001$) in PPH group, whereas it was not significantly correlated with either H/M ($r = -0.28$; $P = 0.16$) or WR ($r = 0.34$; $P = 0.08$) in CTEPH group.

8 were continued on intravenous prostacyclin infusion during the 11 ± 9 mo of follow-up. Kaplan-Meier plots of survival in the CTEPH group and the PPH group are shown in Figure 5. Patients with an H/M < 2.0 had the worse survival in the CTEPH group ($P = 0.016$) and the PPH group ($P = 0.013$) compared with those with an H/M ≥ 2.0.

## DISCUSSION

In this study, we showed that the H/M of $^{123}$I-MIBG and the WR in the left ventricle, which are routinely measured in $^{123}$I-MIBG imaging and are parameters of global LV sympathetic nervous function, reflect the severity of PH, especially in PPH. No patients suffered from hypertension, diabetes mellitus, pheochromocytoma, or Shy-Drager syndrome, which affect the results of $^{123}$I-MIBG imaging (*17*).

Determination of the mechanisms of the abnormal findings of $^{123}$I-MIBG imaging, decreased H/M and increased WR, is still under investigation. An insufficient cardiac sympathetic nerve supply to the LV myocardium and increased activity of the systemic sympathetic nervous system with increased NE turnover are plausible explanations on the basis of animal studies and clinical investigations (*4–10,18*). In this study, organic LV disease was not found on physical examination, echocardiography, or cardiac catheterization in any patients with PH.

In this study, myocardial $^{123}$I-MIBG uptake was decreased in the regions of the septal, anteroseptal, posteroseptal, and posterolateral wall on SPECT images in patients with PH. Morimitsu et al. (*19*) reported that the ratio of $^{123}$I-MIBG uptake in the interventricular septum relative to that in the left ventricle was decreased and that it correlated negatively with mPAP in patients with RV pressure overload. This result complements our findings. It is conceivable that the mechanism of regional myocardial turnover abnormalities is related to the effects of RV overload on LV geometry or right coronary circulation (or both). RV pressure overload in PH can affect not only RV function but also LV function associated with the interaction between the ventricles because the interventricular septum is shared by the ventricles within the closed pericardium (*20–24*). Furthermore, RV hypertrophy in PH, which may cause increased demand for coronary arterial blood flow, can result in a relative shortage of blood supply to the left ventricle.

In this study, the plasma NE concentration, which may reflect abnormality of systemic sympathetic nervous function, was significantly higher in the CTEPH and PPH groups than in the control group. Pulmonary hemodynamic parameters TPR, CO, $Pa_{O_2}$, and $AaD_{O_2}$ were correlated with the plasma NE concentration. Impaired global LV sympathetic function may also be caused by the systemic sympathetic overactivity stimulated by low CO or decreased RV function in PH.

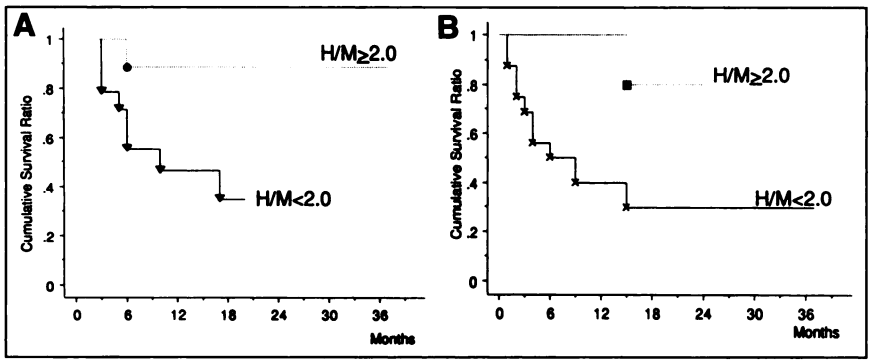


**FIGURE 5.** Kaplan-Meier estimates of survival in patients with H/M ≥ 2.0 and those with H/M < 2.0 in CTEPH group (A) and in PPH group (B). All patients were monitored for at least 6 mo after $^{123}$I-MIBG imaging. Mortality from all causes was used as primary endpoint. Time of death of performing thromboendarterectomy in CTEPH patients and of introduction of continuous intravenous prostacyclin therapy in PPH patients were defined as endpoints. Survival rate of subjects with H/M < 2.0 was significantly lower than that of those with H/M ≥ 2.0 in CTEPH group ($P = 0.016$) and in PPH group ($P = 0.013$).

The H/M and WR, parameters of $^{123}$I-MIBG imaging, were significantly correlated with various pulmonary hemodynamic parameters such as mPAP, TPR, RVEF, and CO in patients with PPH. $^{123}$I-MIBG cardiac imaging may become a useful noninvasive method to assess the severity of PH and to evaluate the effects of therapy in PPH. However, in patients with CTEPH the results of $^{123}$I-MIBG imaging, which correlated only with mRAP, should be used with caution to predict the severity of PH.

The reason for the differing results in the correlation of H/M or WR in $^{123}$I-MIBG imaging with some pulmonary hemodynamic parameters between PPH and CTEPH in this study is unknown. Differences in the patients' age and severity of pulmonary hemodynamic disturbance may be factors. Patients with PPH were younger and revealed worse pulmonary hemodynamic data, represented by mRAP, mPAP, and TPR, whereas those with CTEPH had lower $Pa_{O_2}$ (Table 1). In addition, TPR ranged from 3 to 33 Wood units in CTEPH but from 5 to 42 Wood units in PPH, and RVEF ranged from 13% to 53% in CTEPH but from 10% to 60% in PPH, indicating that the PPH patients had a wider distribution of hemodynamic severity. Furthermore, the older age in patients with CTEPH might affect coronary artery flow and cardiac sympathetic nerve supply to the LV myocardium. These factors could influence the correlation between hemodynamic and $^{123}$I-MIBG imaging parameters.

When the subjects in this study were divided by the cutoff value of H/M = 2.0 in $^{123}$I-MIBG imaging, patients with H/M < 2.0 had poorer survival than did those with H/M ≥ 2.0, in both the CTEPH and the PPH groups. This result indicates that $^{123}$I-MIBG imaging is a noninvasive useful predictor of outcome in patients with pulmonary hypertension. In patients with PPH, it is evident that $^{123}$I-MIBG imaging parameters are very useful in predicting outcome because they showed a strong correlation with most pulmonary hemodynamic parameters. On the other hand, it is conceivable that the significant correlation between $^{123}$I-MIBG parameters and mRAP or RVEF could contribute to the usefulness of the H/M in $^{123}$I-MIBG imaging as an indicator of prognosis in CTEPH patients because mRAP and RVEF are not only parameters of RV function but also important determinants of prognosis in PH.

## CONCLUSION

Our data indicate that patients with PPH and CTEPH may have significant LV myocardial sympathetic nervous dysfunction, which was confirmed by abnormal $^{123}$I-MIBG imaging findings. Furthermore, the parameters of $^{123}$I-MIBG imaging correlated with the severity of pulmonary hypertension, represented by the data from right heart catheterization and cardiac CT. These correlations were more significant in the PPH group than in the CTEPH group. These results suggest that $^{123}$I-MIBG imaging may become a useful and noninvasive modality to determine the severity and prognosis in patients with PPH and CTEPH. Recently, various kinds of effective therapy for PH have been developed. For example, in PPH, long-term therapy with intravenous prostacyclin lowers pulmonary vascular resistance beyond the level achieved in the short term with vasodilating agents (*25*). In CTEPH, pulmonary thromboendarterectomy improves pulmonary hypertension and the quality of life (*26*). As a less invasive method, $^{123}$I-MIBG imaging may also be useful for monitoring the effects of these promising therapies. Further studies are needed to clarify the relationship between autonomic nervous system abnormality and the severity of PH.

## ACKNOWLEDGMENTS

The authors thank the doctors in the Department of Radiology, National Cardiovascular Center, for their valuable advice and also Yoshihiro Nishimura and Tetsuro Katase for their excellent technical assistance. This work was partially supported by the Ministry of Health and Welfare of Japan (grant 9809).

## REFERENCES

1. Moser KM, Auger WR, Fedullo PF. Chronic major-vessel thromboembolic pulmonary hypertension. *Circulation*. 1990;81:1735–1743.
2. Rubin LJ. Primary pulmonary hypertension. *Chest*. 1993;104:236–250.
3. Wieland DM, Wu J-L, Brown LE, et al. Radiolabeled adrenergic neuron-blocking agents: adrenomedullary imaging with I-131 iodobenzylguanidine. *J Nucl Med*. 1980;21:349–353.
4. Wieland DM, Brown LE, Rogers WL, et al. Myocardial imaging with a radioiodinated norepinephrine storage analog. *J Nucl Med*. 1981;22:22–31.
5. Dae MW, Marco TD, Botvinick EH, et al. Scintigraphic assessment of MIBG uptake in globally denervated human and canine hearts: implications for clinical studies. *J Nucl Med*. 1992;33:1444–1450.
6. Stanton MS, Tuli MM, Radtke NL, et al. Regional sympathetic denervation after myocardial infarction in humans detected noninvasively using I-123 metaiodobenzylguanidine. *J Am Coll Cardiol*. 1989;14:1519–1526.
7. Fagre D, Wolf J-E, Vanzetto G, Borrel E. Myocardial uptake of metaiodobenzylguanidine in patients with left ventricular hypertrophy secondary to valvular aortic stenosis. *J Nucl Med*. 1993;34:57–60.
8. Henderson EB, Kahn JK, Corbett JR, et al. Abnormal I-123 metaiodobenzylguanidine myocardial washout and distribution may reflect myocardial adrenergic derangement in patients with congestive cardiomyopathy. *Circulation*. 1988;78:1192–1199.
9. Merlet P, Valette H, Dubois-Rande J-L, et al. Prognostic value of cardiac metaiodobenzylguanidine imaging in patients with heart failure. *J Nucl Med*. 1992;33:471–477.
10. Glowniak JV, Turner FE, Gray LL, et al. Iodine-123 metaiodobenzylguanidine imaging of the heart in idiopathic congestive cardiomyopathy and cardiac transplants. *J Nucl Med*. 1989;30:1182–1191.
11. D'Alonzo GE, Bower JS, Dantzker DR. Differentiation of patients with primary and thromboembolic pulmonary hypertension. *Chest*. 1983;84:679–683.
12. Rich S, Dantzker DR, Ayres SM, et al. Primary pulmonary hypertension: a national prospective study. *Ann Intern Med*. 1987;107:216–223.
13. American Thoracic Society. Standardization of spirometry: 1994 update. *Am J Respir Crit Care Med*. 1995;152:1107–1136.
14. Hajduczok ZD, Weiss RM, Stanford W, Marcus ML. Determination of right ventricular mass in humans and dogs with ultrafast cardiac computed tomography. *Circulation*. 1990;82:202–212.
15. Tada H, Shimizu W, Ohe T, et al. Usefulness of electron-beam computed tomography in arrythmogenic right ventricular dysplasia: relationship to electrophysiological abnormalities and left ventricular involvement. *Circulation*. 1996;94:437–444.
16. Nagaya N, Nishikimi T, Okano Y, et al. Plasma brain natriuretic levels increase in proportion to the extent of right ventricular dysfunction in pulmonary hypertension. *J Am Coll Cardiol*. 1998;31:202–208.
17. Manger WM, Hoffmann BB. Heart imaging in the diagnosis of pheochromocytoma and assessment of catecholamine uptake. *J Nucl Med*. 1993;24:1194–1196.

18. Nakajima K, Taki J, Tonami N, Hisada K. Decreased $^{123}$I-MIBG uptake and increased clearance in various cardiac diseases. *Nucl Med Commun*. 1994;15:317–323.
19. Morimitsu T, Miyahara Y, Sinboku H, et al. Iodine-123-metaiodobenzylguanidine myocardial imaging in patients with right ventricular pressure overload. *J Nucl Med*. 1996;37:1343–1346.
20. Bemis CE, Serur JR, Borkenhagen D, Sonnenblick EH, Urschel CW. Influence of right ventricular filling pressure on left ventricular pressure and dimension. *Circ Res*. 1974;34:498–504.
21. Janicki JS, Weber KT. The pericardium and ventricular interaction, distensibility, and function. *Am J Physiol*. 1980;238:H494–H503.
22. Krayenbuechl HP, Turina J, Hess O. Left ventricular function in chronic pulmonary hypertension. *Am J Cardiol*. 1978;41:1150–1158.
23. Louie EK, Rich S, Brundage BH. Doppler echocardiographic assessment of impaired left ventricular filling in patients with right ventricular pressure overload due to primary pulmonary hypertension. *J Am Coll Cardiol*. 1986;8:1298–1306.
24. Nagaya N, Satoh T, Uematsu M, et al. Shortening of Doppler-derived deceleration time of early diastolic transluminal flow in the presence of pulmonary hypertension through ventricular interaction. *Am J Cardiol*. 1997;79:1502–1506.
25. McLaughlin VV, Genthner DE, Panella MM, Rich S. Reduction in pulmonary vascular resistance with long-term epoprostenol (prostacyclin) therapy in primary pulmonary hypertension. *N Engl J Med*. 1998;338:273–277.
26. Jamieson SW, Auger WR, Fedullo PF, et al. Experience and results of 150 pulmonary thromboendarterectomy operations over a 29 month period. *J Thorac Cardiovasc Surg*. 1993;106:116–127.